MODELLING OF BUBBLE FORMATION WITH THE AID OF CFD

ANDRZEJ K. BIŃ, PIOTR M. MACHNIEWSKI[1]
AND LESZEK RUDNIAK

Department of Chemical and Process Engineering,
Warsaw University of Technology,
Waryńskiego 1, 00-645 Warsaw, Poland

[1] *machniew@ichip.pw.edu.pl*

Abstract: Results of a numerical simulation of the bubble formation process obtained with the aid of computational fluid dynamics (CFD) approach are presented. A solution of the momentum balance (Navier-Stokes) equations was coupled with the volume of fluid (VOF) algorithm for tracking the gas-liquid interface in 2D and 3D domains. The simulation results are compared with the experimental data regarding the influence of gas flow rate on the bubble formation regime and volume of the produced bubbles in a low-viscosity system (air-water). As the simulation results are in agreement with the experimental observations, the VOF algorithm is found to be a valuable tool for studying the phenomena of gas-liquid interaction.

Keywords: bubble formation, cross-flow, CFD, VOF

Nomenclature

d_N [m] – nozzle diameter,
g [m/s^2] – gravitational acceleration,
Q_g [m^3/s] – the gas flow rate,
$\boldsymbol{u}$ – the velocity vector,
α [−] – the gas void fraction.

1. Introduction

Dispersing a gas phase in the form of bubbles is a common way of achieving a high interfacial area in gas-liquid contacting devices (bubble columns, gas-driven loop reactors, stirred gassed tank reactors, *etc.*). This operation is crucial for many industrially important processes like flotation or foam separation and also for those involving mass transfer between gas and liquid phases (aeration of waste, ozonation of potable water, oxidation, *etc.*). The degree of gas dispersion often controls product yield (*e.g.* oxygen absorption rate in a bioreactor) and contactor performance, especially in the cases when a gaseous reactant is consumed in a fast reaction occurring

in the liquid phase (Fleisher *et al.* [1]). The gas is usually sparged by means of a nozzle, a perforated membrane or a porous sparger.

The bubble size distribution in a gas-liquid contactor may depend to a large extent on the initial size of bubbles formed at the gas sparger when the bubbles do not undergo further break-up and coalescence in bubbly dispersion. These conditions are met if the gas phase volume fraction is low ($< 5\%$) so that bubble collisions are rare and bubbles are small enough to survive disruptive inertial or viscous forces in the liquid phase. At higher volume fractions bubble coalescence is retarded if the liquid phase contains electrolytes or trace amounts of surfactants.

In cases when bubble break-up and coalescence cannot be neglected, the resulting bubble size distribution in the two-phase dispersion can be predicted with the aid of the population balance equation (PBE) (Fleisher *et al.* [1], Millies and Mewes [2], Lehr and Mewes [3]). Knowledge of the initial bubble sizes at the gas sparger is necessary for the proper set-up of the macro-distributed PBE. It is also required for the inlet boundary condition necessary to solve the micro-distributed PBE.

Bubble formation is a fairly complicated process influenced by many factors, including properties of the gas and liquid phases (density, viscosity, surface tension), orifice geometry and orientation, the gas flow rate and liquid velocity in the nozzle neighbourhood. The gas flow rate through the nozzle is determined by pressure difference between the growing bubble and the gas chamber on the other side of the nozzle. In the case of small flow resistance in the orifice, variable pressure in the forming bubble causes gas flow variability. The gas chamber pressure also varies unless the volume of the chamber is large enough to damp the pressure fluctuations. This situation is know in the literature as the "constant pressure" regime. On the other extreme, if the pressure drop in the nozzle is greater than pressure fluctuations in the forming bubble, chamber volume no longer influences the process of bubble formation. Thus it is in the "constant flow" regime.

Because of its significance, the bubble formation process has been extensively studied over the last few decades, both experimentally and theoretically (see *e.g.* review paper by Kumar and Kuloor [4]). The models proposed range from approximate (but simple) ones, which assume one- or two-stage growth and detachment of a spherical bubble (Davidson and Schüler [5], Kumar and Kuloor [4]), to more complicated (and realistic) ones, which neither assume a spherical bubble shape nor impose any arbitrary criteria for bubble detachment (see *e.g.* Marmur and Rubin [6], Pinczewski [7], Tan and Harris [8], Terasaka and Tsuge [9], Oğuz and Prosperetti [10]). The application of CFD methods based on numerical solutions of discretised Navier-Stokes equations, coupled with some means of tracking the gas-liquid interface during bubble formation and rise, is relatively new. The possible approaches include methods based on a deformable grid which aligns with the gas liquid interface and follows its movement during the solution (Ryskin and Leal [11]). Other approaches, like the MAC method (Welch *et al.* [12]), are based on fixed grids but introduce artificial marker particles used for tracking the liquid phase during simulation. An alternative technique based on a fixed grid is the VOF (Volume of Fluid) method (Hirt and Nichols [13]), where the volume fraction of one of the phases (usually gas) is treated as the marker

function which, depending on its value (0 or 1), designates a given cell filled with the liquid or the gas phase. The method is known to be computationally more efficient than the MAC method, especially in 3D domains, where one has to follow a large number of tracer particles.

In this work, we have investigated the suitability of the VOF method to realistically simulate the bubble formation process in the constant flow regime.

2. The modelling approach (VOF method)

The VOF model is a fixed-grid technique which uses a single set of momentum equations in the domain shared by both phases. The volume fraction of one of the phases is treated as the marker function and tracked throughout the domain. For this purpose, the continuity Equation (1) for the volume fraction of the phase is solved during the simulation procedure.

$$\frac{\partial \alpha}{\partial t} + \mathrm{div}(\alpha \boldsymbol{u}) = 0. \tag{1}$$

Fluid properties in every cell are calculated additively with respect to the value of this quantity as the average weighed with the volume fraction. Grid cells are filled either with liquid or gas, depending on the value of the void fraction ($\alpha = 0$ or $\alpha = 1$). A cell is considered to contain the interface if the volume fraction of one of the phases is: $0 < \alpha < 1$. Special algorithms were developed to prevent smearing of the interface over several neighbouring cells due to numerical diffusion. Due to discretisation and interpolation errors in calculating volume fraction fluxes between computational cells it is necessary to use grids sufficiently fine to ensure volume conservation of the phases (provided incompressibility of both phases is assumed).

The VOF method was used by Delnoij *et al.* [14] and Krisha and van Baten [15] to simulate a 2D bubble rising in a stagnant liquid. They found fair agreement of the simulated bubble shape and rise velocity with experimental observations. Recently, van Wachem and Schouten [16] have applied the VOF method with the piecewise-linear geometric reconstruction of the interface (PLIC VOF) developed by Youngs [17] to simulate the rise of a single 3D bubble (1–5 cm in diameter) in a rectangular column and obtained favourable agreement with experimental results.

3. The simulation procedure

The simulation was performed with the aid of the FLUENT 6.1 CFD code, using the Finite Volume approach (Patankar [18]) for discretisation of the mass, momentum and void fraction balance equations on unstructured computational meshes. A second-order upwinding scheme was used to calculate the convective terms. Both phases were treated as incompressible and the SIMPLE method was used for pressure-velocity coupling (Patankar [18]). The position of the interface between the gas and the liquid was calculated using the Volume of Fluid model (VOF) with piecewise-linear geometric reconstruction of the interface (PLIC VOF, Youngs [17]). Time dependence was resolved in an implicit marching scheme by iterating in time with a constant time step. Contrary to momentum equations, Equation (1) was integrated using an explicit time marching scheme. In order to ensure numerical stability, the time step was internally subdivided to meet the Courant number criterion.

Surface tension was accounted for in the simulation. The resulting force was modelled as an additional source term in the momentum equation, dependent on the local curvature of the interface (the CSF model by Brackbill *et al.* [19]).

Selected properties of the phases used in the simulation are presented in the Table 1.

Table 1. Properties of the fluids used in the simulation

Property	Liquid (water)	Gas (air)
density [kg/m^3]	998.2	1.225
viscosity [Pa·s]	$1.003 \cdot 10^{-3}$	$1.7894 \cdot 10^{-5}$
surface tension [N/m]	0.073	

The simulation illustrated the process of bubble formation in a stagnant liquid from an orifice 0.3 mm in diameter held horizontally. The gas was supplied to the orifice via a 4 mm long capillary (nozzle) of the same diameter at a constant rate in order to mimic the constant flow coditions. Two modeling approaches were applied:

- axial symmetry was assumed and the problem was solved in a 2D domain,
- no symmetry was assumed, which required a full solution in a 3D domain.

3.1. Approach A

The axisymmetric computational domain (2D) is shown in Figure 1. The domain extends 5 mm in the radial direction and 24 mm in the axial direction (including the 4 mm long nozzle, 0.3 mm in diameter). The "symmetry" boundary condition was set at the axis (zeroing of momentum, mass and void fraction fluxes in the radial direction) and a constant pressure of 101 325 Pa was set as a boundary condition at the outlet from the domain. In order to stabilize the bubble's attachment point to the edge of the orifice, a zero static contact angle of the liquid at the bottom wall (*i.e.* good wettability of the orifice plate and poor wettability of the nozzle wall) was set as the boundary condition for determination of interface shape at the attachment point.
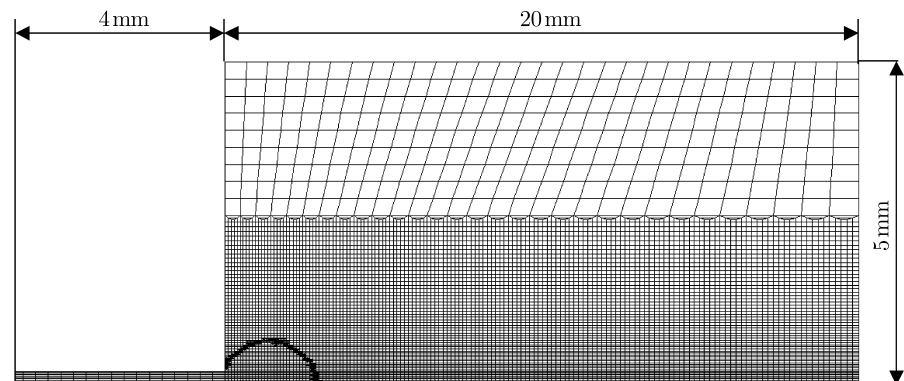

Figure 1. Schemat of the 2D computational domain and the adopted grid corresponding to the interface at a sample time instant

The mass flow rate of the gas phase was set as a boundary condition at the inlet of the nozzle. Three different gas mass flow rates were investigated: $2 \cdot 10^{-8}$ kg/s, $1 \cdot 10^{-7}$ kg/s, $1 \cdot 10^{-6}$ kg/s (corresponding to volumetric flow rates: 0.0163 mL/s, 0.0816 mL/s and 0.816 mL/s, respectively).

The grid used in the simulation consisted of approximately 10 000 quadrilaterals and was refined during the solution procedure for better resolution of the interface between the fluids. Values of the normalized void fraction gradient were used as the grid adoption criteria.

The solution was obtained in an unsteady manner with a time step of $1 \cdot 10^{-6}$ s in the case of the two lower gas flow rates and $1 \cdot 10^{-7}$ s in the case of the highest gas flow rate.

3.2. Approach B: simulation in a 3D domain

A schemat of the computational domain is shown in Figure 2. The geometry was cylindrical with a diameter of 3 cm and a height of 2 cm (excluding the nozzle, 4 mm long and 0.3 mm in diameter). The grid consisted of over 115 000 hexahedral cells and, due to limitations of the computing time, had to be much coarser than that in the 2D approach. The mesh was finer in the neighbourhood of the orifice so that the perimeter of a forming bubble on the lateral cross-section always consisted of approximately 50 cells. Mesh adoption was abandoned because the computing times grew prohibitively high (72 hours of computing time on an Intel Xeon 2.8 GHz
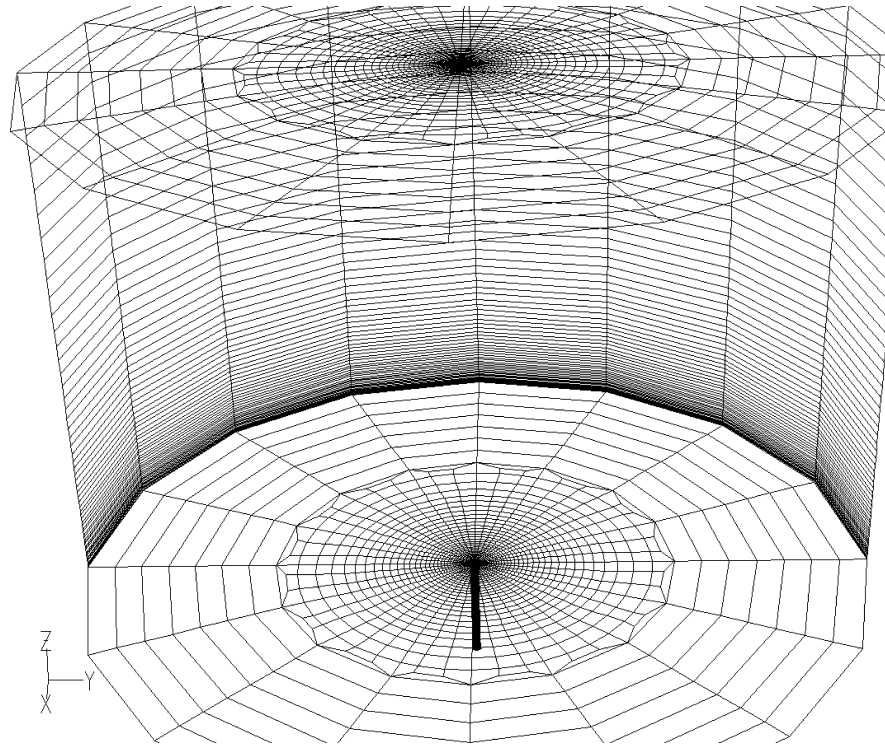
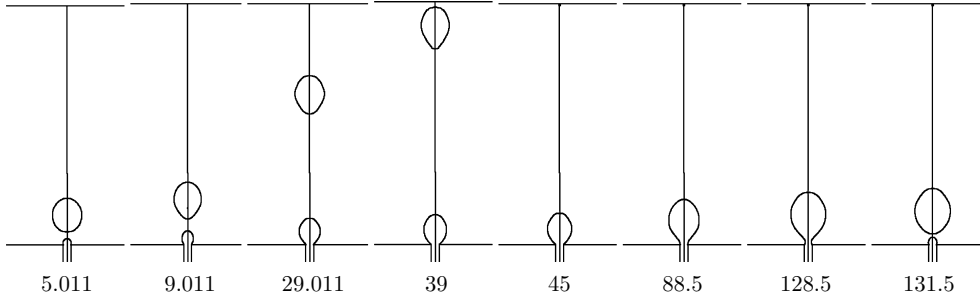

Figure 2. Schematic view of the 3D computational grid

Figure 3. Simulated interface during axisymmetric bubble growth (single bubbling regime, $Q_g = 0.0163 \, \text{mL/s}$); the numbers indicate relative time in milliseconds
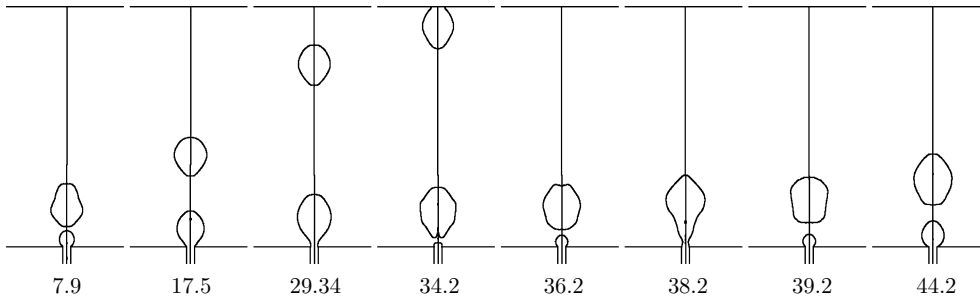

Figure 4. Simulated interface during axisymmetric bubble growth at gas flow rate (incipient bubble pairing, $Q_g = 0.0816 \, \text{mL/s}$); the numbers indicate relative time in milliseconds

3-processor cluster per aproximately 1 ms of flow time). Boundary conditions were similar to those in the 2D case, except for the axis.

Only one gas mass flow rate of $1 \cdot 10^{-6} \, \text{g/s}$ was investigated for comparison with the 2D approach. A constant pressure of $101\,325 \, \text{Pa}$ was set as a boundary condition at the top of the domain. The solution was obtained in an unsteady manner with a time step of $1 \cdot 10^{-6} \, \text{s}$.

4. Results

Contours of the void fraction equal to 0.5, which indicate the location of the gas-liquid interface, are shown in Figures 3–5 for different time instants. Single bubbling was observed only for the smallest gas flow rate, $Q_g = 0.0163 \, \text{mL/s}$ (Figure 3). In the case of higher flow rates, the results indicated coalescence of two or more primary bubbles (see Figures 4 and 5). This is in accordance with experimental observations. According to Walters and Davidson [20], incipient bubble pairing occurs for

$$Q_g > C g^{1/2} d_N^{5/2}, \tag{2}$$

where C takes values from 1.3 to 6.2. Wraith [21] suggests the value of $C = 7.44$.

Equation (2) predicts the critical gas flow rate in the modelled system equal to $0.0363 \, \text{mL/s}$.

For the highest simulated gas flow rate ($Q_g = 0.816 \, \text{mL/s}$), gas momentum has significant influence on the bubble formation process. The tip of the forming bubble is clearly distorted in Figure 3 (*e.g.* $t = 9.125 \, \text{ms}$) by the gas jet emerging from the orifice. It is also evident from the figure that the closing bubble neck is immediately destroyed
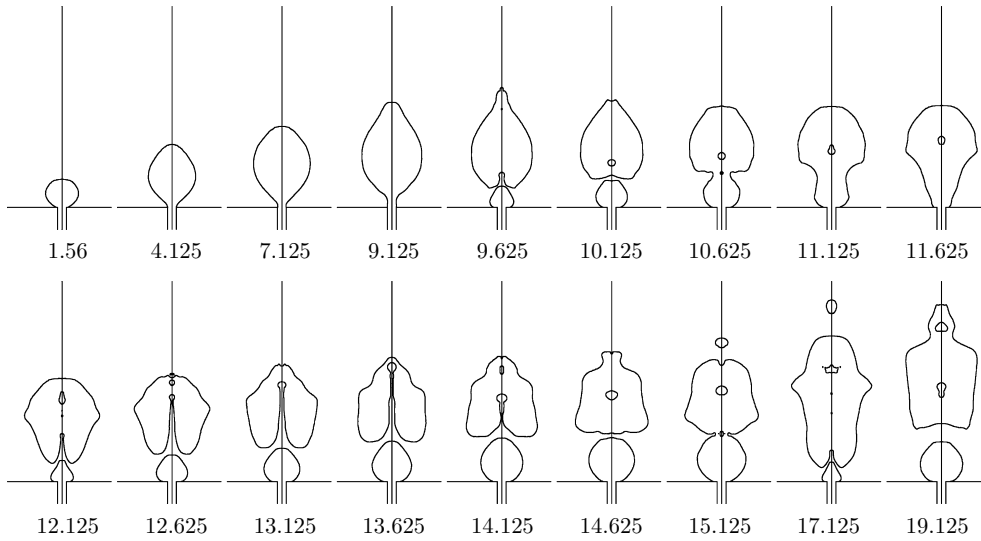
Figure 5. Multiple incipient coalesce during axisymmetric bubble growth; the numbers indicate time in milliseconds elapsed after starting the gas flow through the nozzle ($Q_g = 0.816 \, \text{mL/s}$)
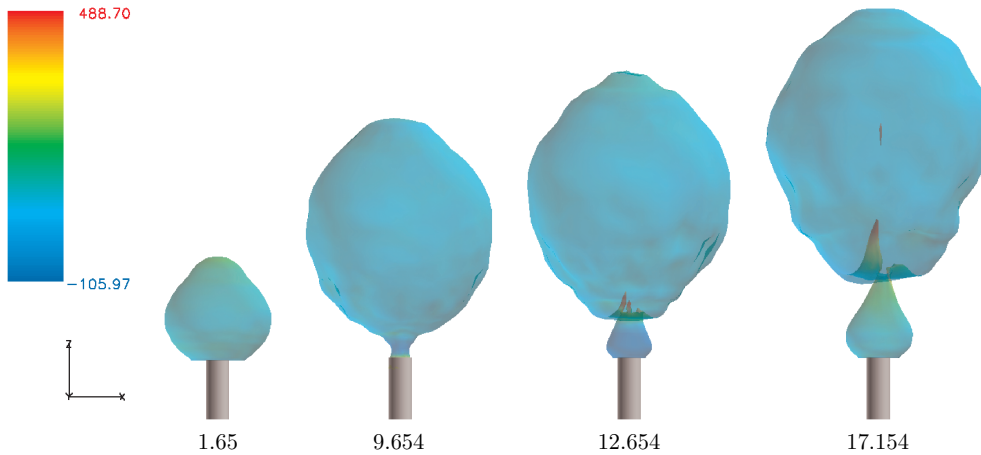

Figure 6. The interface during bubble growth at gas flow rate $Q_g = 0.82 \, \text{mL/s}$ (3D approach); numbers indicate time in milliseconds elapsed after starting the gas flow; colours indicate static pressure relative to $101\,325 \, \text{Pa}$

causing ejection of secondary droplets inside the bubble and initiating a capillary wave travelling along the bubble's envelope. It can be observed that the clashing capillary wave at the top of the bubble ejects small secondary satellite bubbles from the forming bubble's top. This phenomenon has also been observed and reported lately by Tse *et al.* [22], with regard to coalescing bubbles in a bubbly dispersion.

Sample results of the 3D simulation are presented in Figures 6 and 7. Due to the coarser grid, the shape of the interface could not be resolved in such high detail as that in the 2D simulation. Nevertheless, similarly to the 2D case, the bubble shape is highly distorted, but the axial symmetry is lost shortly after bubble detachment, resulting in the well-know meandering movements during rising of the formed bubbles (Figure 7).
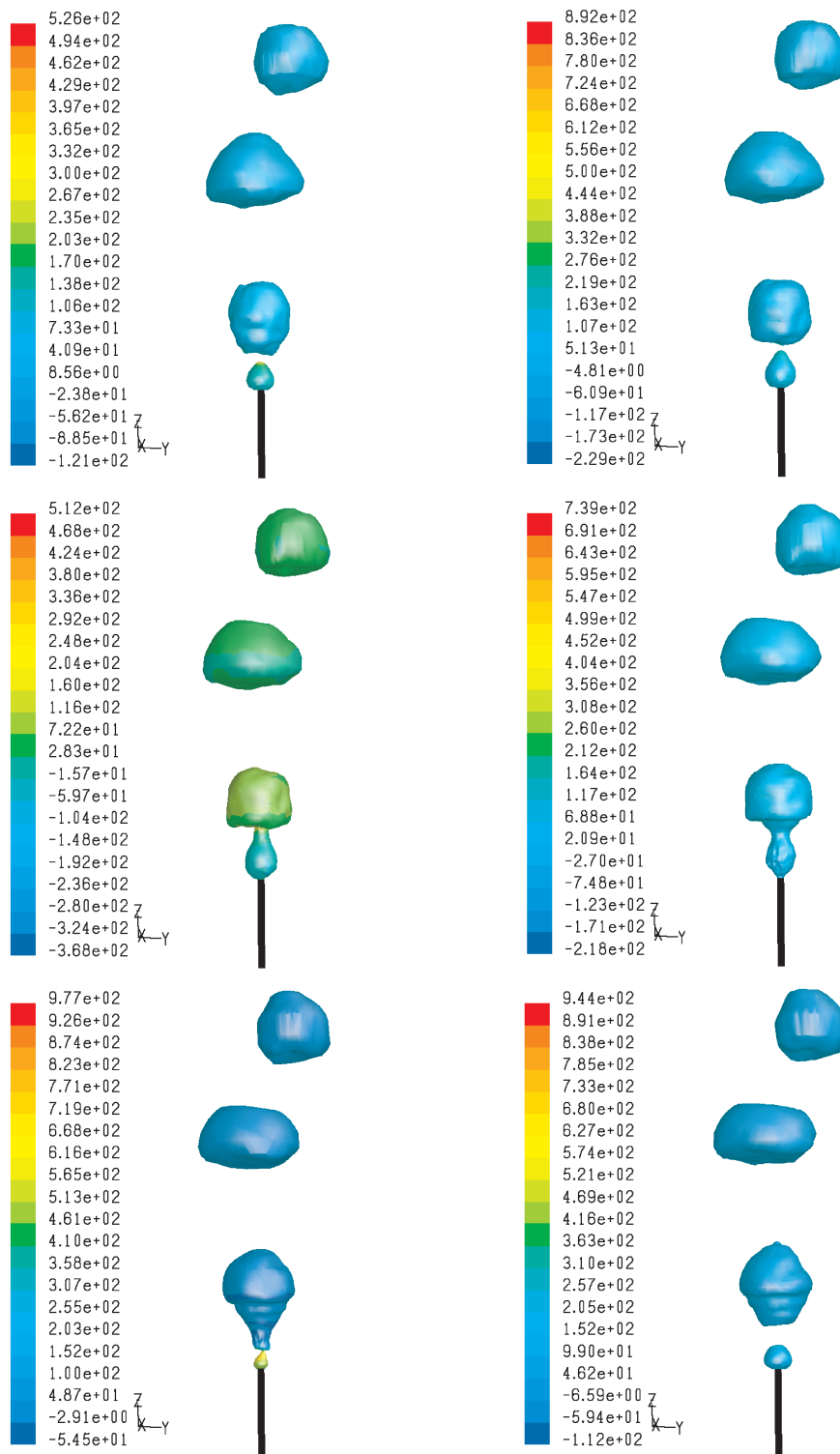
Figure 7. The interface during 3D bubble growth and rise at time instants 1 ms apart; colours indicate static pressure relative to 101 325 Pa

Figure 8. Incipient coalescence of bubbles during bubble formation from an orifice 0.3 mm in diameter; average gas flow rate – 0.83 mL/s; time resolution – 1000 fps
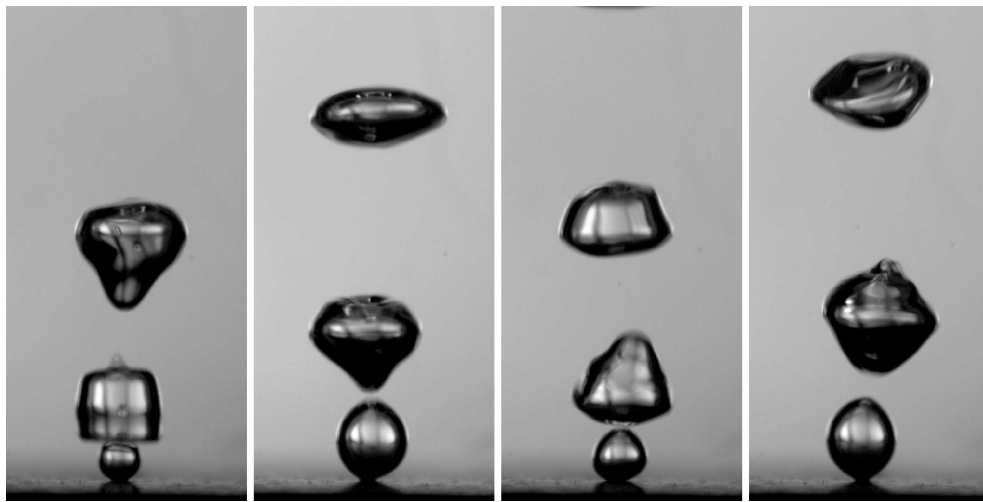

Figure 9. Incipient coalescence of bubbles during bubble formation from an 0.3 mm orifice; average gas flow rate – 0.83 mL/s; close-up, time resolution – 60 fps

In order to compare the simualtion results with exeprimental observations, the process of bubble formation in distilled water was visualised with the aid of a high speed camera. The details of the experimental setup are reported elsewhere [23].

Constant flow conditions are difficult to obtain experimentally for very small gas flow rates, as the volume of the capillary that delivers the gas acts as a gas chamber. Therefore, comparison with experimental data was only possible for the highest simulated flow rate ($Q_g = 0.816$ mL/s). The volume of the simulated bubbles formed in this case was on the average equal to 26 mm^3. This value is in agreement with experimental data within the 10% error connected with data scatter.

Also the shapes of the simulated bubbles during incipient coalescence clearly resemble those observed experimentally (*cf.* Figures 8 and 9).

Regarding the issue of volume conservation of the VOF algorithm, the calculated ratio of the total gas volume in the domain per time was equal to the gas flow rate at the nozzle inlet, with accuracy better than 0.015%.

5. Conclusions

We have investigated the ability of the VOF method to simulate the bubble formation process in a constant flow regime. As the computational mesh needs to

Andrzej K. Biń et al.

be sufficiently fine for the VOF technique to perform well, its application to simulate 3D phenomena generated a substantial load for computing devices. Nevertheless, the results obtained in this work are very encouraging and prove that application of the VOF method enables one to achieve greater fidelity and detail in studying the phenomena of gas-liquid interaction in a wide range of parameters.

Acknowledgements

References

[1] Fleisher C, Becker S and Eigenberger G 1996 *Chem. Eng. Sci.* **51** (10) 1715
[2] Millies M and Mewes D 1999 *Chem. Eng. & Proc.* **38** 307
[3] Lehr F and Mewes D 2001 *Chem. Eng. Sci.* **56** 1159
[4] Kumar R and Kuloor N R 1970 *Adv. Chem. Engng.* **8** 255
[5] Davidson J F and Schüler B O G 1960 *Trans. Instn. Chem. Engrs.* **38** 335
[6] Marmur A and Rubin E 1976 *Chem. Eng. Sci.* **31** 453
[7] Pinczewski W V 1981 *Chem. Eng. Sci.* **36** 405
[8] Tan R B H and Harris I J 1986 *Chem. Eng. Sci.* **41** (12) 3175
[9] Terasaka K and Tsuge H 1993 *Chem. Eng. Sci.* **48** (19) 3417
[10] Oğuz H N and Prosperetti A 1993 *J. Fluid Mech.* **252** 111
[11] Ryskin G and Leal L G 1984 *J. Fluid Mech.* **148** 19
[12] Welch J E, Harlow F H, Shannon J P and Daly B J *The MAC Method: A Computing Technique for Solving Viscous Incompressible Transient Fluid Flow Problems Involving Free Surfaces*, Los Alamos Scientific Laboratory Report, LA-3425
[13] Hirt C W and Nichols B D 1981 *J. Comput. Phys.* **39** 201
[14] Delnoij E, Kuipers J A M and van Swaaij W P M 1997 *Chem. Eng. Sci.* **52** 3623
[15] Krishna R and van Baten J M 2001 *Chem. Eng. Technol.* **24** (4) 427
[16] van Wachem B G M and Schouten J C 2002 *AIChE J.* **48** (12) 2744
[17] Youngs D L 1982 *Numerical Methods for Fluid Dynamics* (Morton K W and Baines M J, Eds), Academic Press, p. 273
[18] Patankar S V 1980 *Numerical Heat Transfer and Fluid Flow*, Hemisphere, Washington, D.C.
[19] Brackbill J U, Kothe D B and Zemach C 1992 *J. Comput. Phys.* **100** 335
[20] Walters J K and Davidson J F 1962 *J. Fluid Mech.* **12** 408
[21] Wraith A E 1971 *Chem. Eng. Sci.* **26** 1659
[22] Tse K L, Martin T, McFarlane C M and Nienow A W 2003 *Chem. Eng. Sci.* **58** 275
[23] Biń A K, Machniewski P M and Rudniak L 2004 *Modelling Bubble Formation in Stagnant and Cross-flowing Liquids* to be published in *Inżynieria Chemiczna i Procesowa*